A MODEL STUDY OF BUOYANT JETS

by

HWACHII LIEN

B. S., National Taiwan University, Taipei,
Taiwan, China, 1953

A THESIS

submitted in partial fulfillment of the

requirements for the degree

MASTER OF SCIENCE

Department of Mechanical Engineering

KANSAS STATE COLLEGE
OF AGRICULTURE AND APPLIED SCIENCE

1956

TABLE OF CONTENTS

INTRODUCTION

Many exploratory studies have been made in the Engineering Experiment Station of Kansas State College pertaining to the stream of a downwardly projected jet of air. The equations have been formulated for throw, L/D_o, in terms of the buoyancy number $(U_o^2/gD_o)/\left[(\bar{\rho}_a/\bar{\rho}_o)-1\right]$, and many experimental data supporting the equation have been presented in three papers (4, 5 and 6).

Of primary interest in the study of jet-diffusion are the temperature distribution, momentum change, and the transport of material. Of these three, material transport has been the most neglected one. Furthermore, because of difficulties inherent in the use of liquids, most of the experimental work has been with gases. A paper by Forstall and Gaylord (3) recently reported that the behavior of an unheated water jet was quite similar to that of an unheated air jet. They concluded that: (1) the behavior of the water jet was the same as that found by others for an air jet issuing into air, and hence constants obtained from measurements in air can be applied to water, (2) the turbulent Schmidt number $(\mu/\rho D_v)$ for water is approximately equal to the turbulent Schmidt number for air, and (3) the error curve [1] serves as a useful and satisfactory representation of diffusion profiles for water just as it does for air.

The purpose of the experiment was to investigate the charac-

---

[1]

$$U_c/U_o = e^{-0.694(r/r_n)^2}$$

where r_n is the value of r where the respective value of U_c/U_o reaches 1/2.

teristics of a jet of heated water projected vertically downward into a bath of unheated water, and to relate these to corresponding data on downwardly projected jets of heated air. Specifically, the objectives of the study were to (1) obtain data descriptive of the behavior of the downwardly projected jet of heated water, (2) investigate the establishment and location of the jet boundary by the shadow graphs or potassium per manganese technique, (3) compare the data or downthrow of water jets to that of the air jets, (4) find out the buoyancy force of the water jet by graphical integration and check with the change of momentum flux at the jet, (5) obtain guidance for further research.

BASIC CHARACTERISTICS OF HEATED FLUID JETS

The mixing pattern of round jets entering a stationary fluid of the same density is shown in Fig. 1, Plate I. It must be noted that the inverted conical region in this figure is the so-called primary zone of the jet. As the fluid flows out of the outlet, it begins to entrain the stationary surrounding fluid. But the entrained air does not reach the axis of the stream until the apex of the conical region is formed. This primary zone also can be characterized by a center line velocity which remains approximately the same as the velocity of the fluid at the center of the outlet. The end of the primary zone is the beginning of the principal zone. This principal zone is marked by a decrease in the center-line velocity. This velocity decrease is due to the turbulent mixing of the fluid from the nozzle and the surrounding fluid which is entrained by the moving stream (Corrsin, 2). The major portion of

EXPLANATION OF PLATE I

Fig. 1. Sketch illustrating nomenclature.

Fig. 2. Showing all the forces acting on the tank.

PLATE I

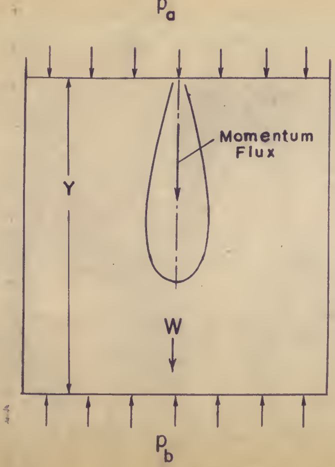

Fig. 2

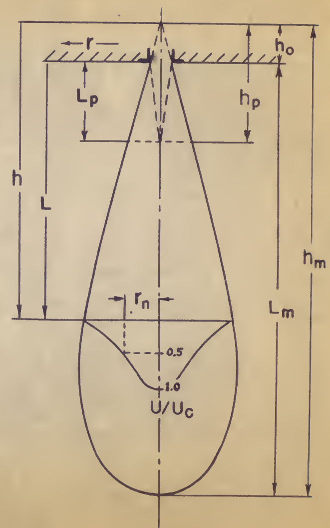

Fig. 1.

the water jet studied was included in this zone; thus most of the data presented in this thesis represent the characteristics of this zone. Various investigators have found that the boundary between the primary and principal zones formed at a distance of approximately 5 nozzle-diameters below the nozzle outlet. At this distance from the nozzle the turbulent mixing of the fluid has penetrated to the center line of the fluid stream (Albertson et al., 1).

The lowest region in the stream has been defined as the terminal zone. In this zone the fluid stream is in a completely turbulent state. The bottom of the jet boundary can not be well established, as it continually changes because of the high turbulence.

For the downward projection of heated air, Helander and Yen of Kansas State College developed the following formulas:

1. Velocities along the vertical axis of the jet (center-line velocities) in the principal zone would be represented by an equation below with n between 1/2 and 1/3.

$$U_c/\bar{U}_o = \frac{h_p}{h}\left[\frac{1-(h/h_m)^2}{1-(h_p/h_m)^2}\right]^n$$

2. Temperatures along the vertical axis of the jet in the principal zone would be represented by an equation:

$$\frac{T_c - \bar{T}_a}{\bar{T}_o - \bar{T}_a} = \frac{h_p'}{L+h_o'} = \frac{h_p'/D_o}{h'/D_o}$$

The author with Knaak studied downwardly projected jets of heated air from a 4" A.S.M.E. nozzle and obtained the following empirical formulas (7):

$$\frac{L_p}{D_o} = \left[\frac{172}{1 + \frac{172}{(L_m + 7.5)^2}}\right]^{\frac{1}{2}} - 7.5 \quad \text{where } L_m = 1.41\sqrt{\bar{B}_o}$$

$$h_p/h_m = \frac{84.4}{\bar{B}_o + 138} + 0.066$$

$$h'_p/D_o = 1.482 \cdot \bar{B}_o^{0.14}$$

$$h'_o/D_o = \frac{4359}{\bar{B}_o + 821} - 0.51$$

BASIC THEORY

A major purpose of this research was to determine whether or not the change of momentum flux equaled the buoyancy force. To do this, two different ideas were applied as indicated below:

1. From the requirement for the equilibrium of forces in Fig. 2, Plate I, after the establishment of the jet boundary:

$$p_a \cdot A + (M_o \cdot U_o/g_c) + W - p_b \cdot A = 0$$

or

$$(p_b - p_a)A + W = (M_o \cdot U_o/g_c)$$

and assume that the temperature gradient over the entire depth of the cold water bath be negligible at a distance remote from the jet, then

$$p_b = Y\rho_a + p_a \quad \text{thus,}$$

$$-AY/\rho_a + W = (M_o U_o/g_c) \quad \text{and also,}$$

$$W = AY\int_0^{V_b} \frac{dV}{V_b} \quad \text{thus,}$$

$$(M_o \cdot U_o/g_c) = AY(\rho_a - \int_0^{V_b} \frac{dV}{V_b}) \quad \text{------------ (A)}$$

It can be easily seen that $AY(\rho_a - \int_0^{V_b} \frac{\rho dV}{V_b})$ is equal to reduction of the weight of the water in the bath due to the heated water which was distributed non-uniformly within the bath. This can be determined by $\int_0^{V_j'} (\rho_a - \rho)\, dV$, where the jet boundary in this case must be defined as the enclosed surface of zero temperature difference with the surrounding water. A conclusion obtained by the formula (A) is that the "buoyancy force developed by the heated water jet must be equal to the momentum flux at the outlet"; or

$$(M_o \cdot U_o/g_c) = \int_0^{V_j'} (\rho_a - \rho)\, dV = F_b$$

2. Another attempt to reach the above conclusion was made by measuring the time for the complete establishment of the jet boundary. If we treat the water injected in time as producing the buoyancy force that counteracts the momentum flux, M_oU_o:

$$\frac{M_o g\, \theta}{g_c \rho_o} (\rho_a - \rho_o) = F_b = (M_oU_o/g_c) \quad \text{thus:}$$

$$\theta = \frac{U_o}{g \cdot \frac{(\rho_a - \rho_o)}{\rho_o}} \qquad \text{------------------(B)}$$

If the buoyancy force developed by the heated water jet be equal to its initial momentum flux, then θ measured experimentally as the time required for the initially emerging jet to realize its maximum downward travel should be equal to the value obtained by the formula (B).

DESCRIPTION OF TEST EQUIPMENT

The general components of the equipment used are shown in

EXPLANATION OF PLATE II

View of general set-up showing heating devices, Brown indicator, potentiometer, powerstat, water tanks, drain tubes, pitot tube, thermocouples, and a micro-manometer (*)

PLATE II

Plate II. It consisted of a heating device, a Brown thermometer as a control indicator, a 0.159-inch nozzle, a powerstat, indicating instruments, an upper water container, and a main vessel.

Water was introduced first to the upper water container. The level of water in this container was then regulated by a drain tube to keep a constant height. Water from the upper container was projected downwards through a 0.159-inch nozzle into the cold bath. There was a stop valve between the container and the nozzle to stop the flow whenever it was necessary to restore the test conditions, to heat up the water in the upper container, or to discontinue the test. A drain tube also was attached to the cold bath for the purpose of maintaining a constant level in the bath and the flow rate was measured from the drainage.

Plate III shows the dimensions and the schematic arrangement of the water container and the main vessel. The vessel was made of galvanized sheet metal except that a large glass plate was used for a front wall so as to make observations through the water possible.

Plate IV is a view of the instrument carriage showing the thermocouple and the pitot tube extending out from the carriage. There was pair of racks on the top of the bath container by which the carriage was moved to its proper horizontal measuring position. The vertical movement of the pitot tube and the thermocouple was obtained by merely turning a pulley to let them slide along a vertical guide. This enabled one to bring the pitot tube and the thermocouple to any desired position below the nozzle. In the immediate vicinity of the outlet, the pitot tube and the

EXPLANATION OF PLATE III

Schematic drawing of water tanks, etc.

1. Heater 2. Drain tube 3. Upper tank

4. Valve 5. By pass to maintain temperature in nozzle head when jet is shut off

6. Instrument carriage 7. Water level

8. Drain tube 9. Pitot tube 10. Thermocouple

11. Thermocouple junctions to detect the average reference temperature of surrounding water

12. Main water container 13. Front glass

14. Drain valve

PLATE III

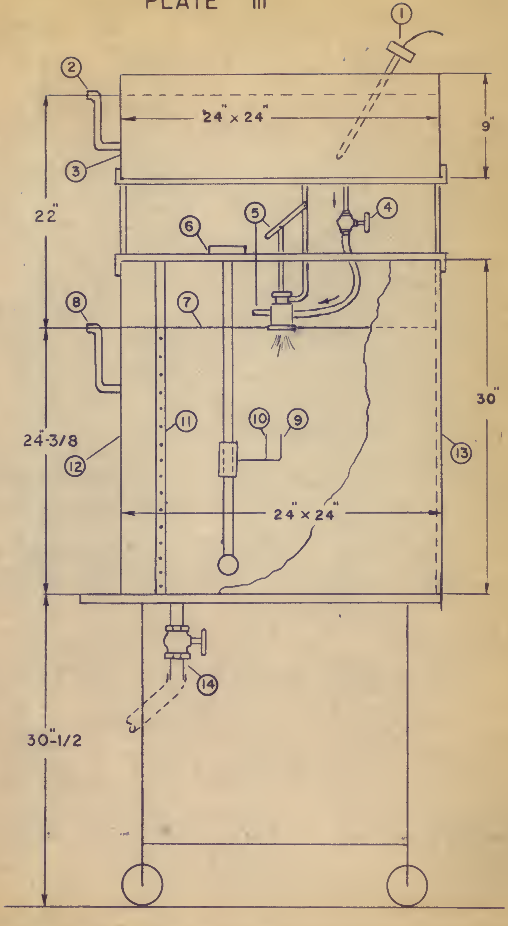

EXPLANATION OF PLATE IV

Close-up view of instrument carriage

PLATE IV

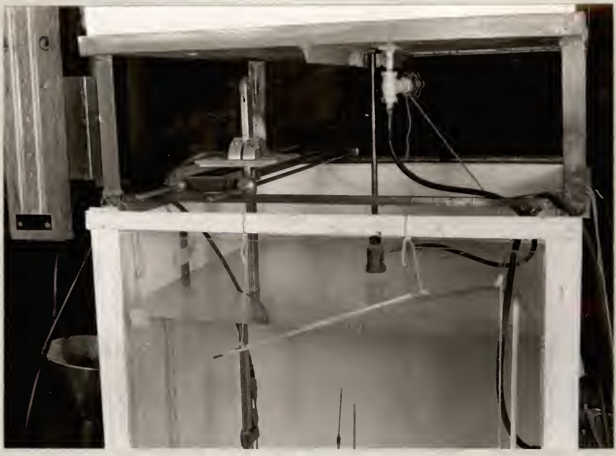

thermocouple to any desired position below the nozzle. In the immediate vicinity of the outlet, the pitot tube and the thermocouple could not, with this equipment, be brought accurately to the desired position. The diameter of the nozzle and the required increment of movement for making measurement in the region were so small that even a slight inaccuracy caused a large error. An inaccuracy in the measuring position of 1/64 inch was possible, and this possible error was nearly 10 per cent of the orifice diameter.

Water was heated up by the two 500-watt and one 1000-watt immersion heaters. The amount of the water in the upper tank was so large that it would have taken more than two hours to heat all of it to the desired temperature. Because of this, an open-ended wooden box in the form of a vertical channel was placed around the heating element so as to limit the amount of water heated to that confined within the box. Water for the nozzle was then drawn off from the upper region of the enclosed surface by means of a vertical pipe as shown in Fig. 1, Plate V. Water entered the channel through an opening near the bottom of the channel. With this arrangement, it took only a few minutes to heat up the water to the desired temperature.

During the test, it was essential that the temperature difference[1] be kept constant. A discussion of the arrangement used to meet this requirement appears in a later chapter.

The velocity was measured mostly by a pitot tube of 0.046

---

[1]The difference between the temperature of the water at the nozzle outlet and that of the surrounding water in the tank remote from the jet.

inch inside diameter made from a hypodermic needle.[1] Though much slower in its response, a smaller hypodermic needle of 0.020 inch inside diameter was used in the vicinity of the nozzle outlet when greater accuracy was required than that obtainable with a 0.046-inch diameter opening. A well-finished base was connected to the end of the tube stem. This made the interchange of the needles easy.

INSTRUMENTATION

Measurement of Velocity

The velocity measurement was quite difficult in this experiment because the values of the velocities were very small. At first, an inclined manometer was introduced. It was supposed to expand the scale so that the head might be read more accurately. But it was not successful because of a very slow response. This slow response was due to the surface tension of the water in the inclined tube and also to the small pressure differentials being measured. For the next trial, a liquid column U tube manometer was employed. In order to expand the scale, it was desirable to use a manometric liquid with a density slightly greater than that of water. It was calculated that the specific gravity of the liquid should be nearly 1.10; Marriam instrument red oils with the specific gravities of 0.86 and 3.23 were combined to make the required liquid. After several tests with this liquid, it was decided to give up the using of this liquid column U tube manome-

[1] Measurement of Velocity.

ter as the response was very slow and the indications were uncertain. Trials with gasoline as the manometric liquid were made, but also failed. A final decision was made to use a simple micromanometer as shown In Plate II. This was merely a water column U tube with a screw adjustment for fine reading. Strictly speaking, this was not an ideal instrument, and some other means are needed for future experiments.

Measurement of Temperature

At a distance one inch from the pitot tube, a thermocouple junction was installed. By a carriage arrangement shown in Plate IV it was possible to move this thermocouple junction either horizontally or vertically to any position desired for the measurement of temperature. The thermocouple was connected to a potentiometer. The thermocouple wires used were No. 30 B. & S gauge copper and constantane.

TESTING CONDITIONS AND PROCEDURE

Since it was not possible to make all measurements simultaneously, the test conditions had to be kept exactly the same during one complete run. It was easy to regulate the height of water in both the upper and the lower tanks by merely using the drain tubes as shown in Plate III. There were two much more difficult problems: how to keep a constant difference between the temperature at the nozzle outlet and that of the water in the bath remote from the outlet, and how to compensate for the effect of the vertical temperature gradient in the bath. Hot water from the nozzle tended to accumulate on the surface of the bath and thus caused the vertical temperature gradient to become steeper and steeper.

In order to keep a constant difference between the temperature of the water at the nozzle outlet and that of the water in the bath remote from the jet, a powerstat regulation of the heater voltage was introduced quite successfully with the help of automatic indication of the temperature difference by means of Brown thermometer. This arrangement is shown schematically in Fig. 2, Plate V. The temperature of the surrounding water was not uniform due to the hot water accumulation on the surface, so the average temperature in a vertical column near the wall of the bath was taken as the reference temperature. This average temperature was measured by ten thermocouple junctions spaced two inches apart vertically and connected in a parallel. Then by these junctions connected in series with another junction at the nozzle outlet, the temperature difference was detected as a potential difference. These thermocouple leads were connected to the Brown indicator so that any slight change of the temperature difference was observed by the movement of the indicator needle. Whenever the needle of the indicator tended to move, the powerstat was adjusted to change the heater voltage so as to keep the temperature difference always constant.

The temperature gradient along the depth varied with time and made the test conditions quite unsteady. The bad effect of this unsteady condition was somewhat eliminated by periodically draining the hot water from the main vessel, and replacing it by

EXPLANATION OF PLATE V

Fig. 1. Schematic drawing showing the arrangement for quick heat-up.

1. Heater
2. Water level
3. Hot-water guide pipe
4. Open-ended wooden box

Fig. 2. Schematic wiring diagram for temperature control-indication

1. Heater
2. Upper tank
3. Thermocouple junction at nozzle outlet
4. Ten thermocouple junctions to detect the average reference temperature of surrounding water
5. Main water container
6. Powerstat
7. Brown indicator

Thermocouple wires

Constantan ____.______.____

Copper ______________

PLATE V

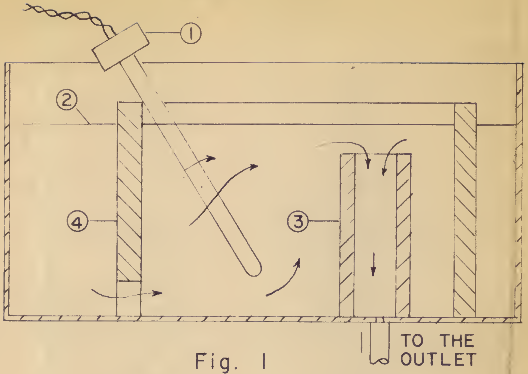

Fig. 1

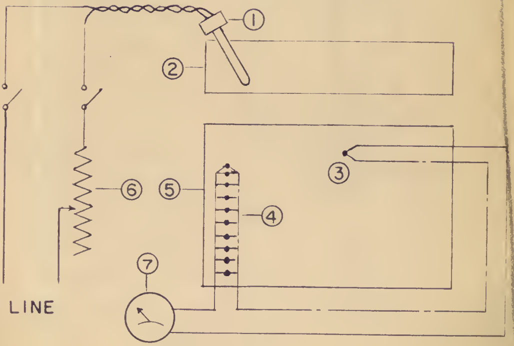

Fig. 2

fresh cold water so as to restore original condition after a sufficient stirring and settling. This was done each time the instrument carriage was moved to a new level.

Two complete runs were made with temperature differences of 33° F. and 47° F., respectively. The velocity and temperature distributions were measured over the entire region of the jet. The jet boundaries were traced quite accurately by means of shadow graphs.[1] Flow rates were measured by measuring the drainage in a measured time.

DATA AND RESULT

Two separate runs with duplicate measurements for each point gave data from which the temperature and velocity profiles were plotted. Although broad generalizations could not be drawn from the data obtained, the similarity of the water jet to the air jet was evident.

Velocity Profiles

The complete sets of data obtained by velocity measurement are shown as velocity profiles in Plates VI and VII, for $\bar{B}_o$ = 1568 and $\bar{B}_o$ = 2450. These cross jet velocity profiles obtained at representative levels have been plotted on common dimensionless coordinates of L/D_o and r/D_o. The main purpose of the set of profiles is to give a graphical picture of the air stream instead of qualitative treatment of the stream. From these curves, error function, $U/U_c = e^{-cx^2}$, curves were obtained as shown in Plates

[1] See Plate XVI.

EXPLANATION OF PLATE VI

Velocity Profiles

$\bar{B}_0 = 1568$

PLATE VI

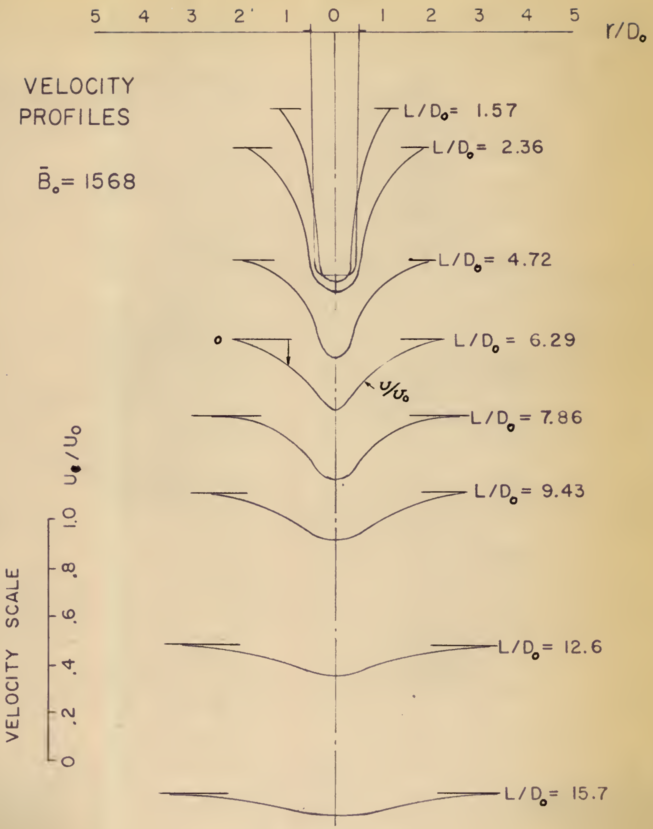

5 4 3 2 1 0 1 2 3 4 5
r/D₀
VELOCITY
PROFILES
B̄₀= 1568
L/D₀= 1.57
L/D₀= 2.36
L/D₀= 4.72
L/D₀ = 6.29
0
U/U₀
L/D₀ = 7.86
L/D₀= 9.43
L/D₀= 12.6
L/D₀= 15.7
U/U₀
VELOCITY SCALE
0 .2 .4 .6 .8 1.0

EXPLANATION OF PLATE VII

Velocity Profiles

$\bar{B}_o = 2450$

PLATE VII

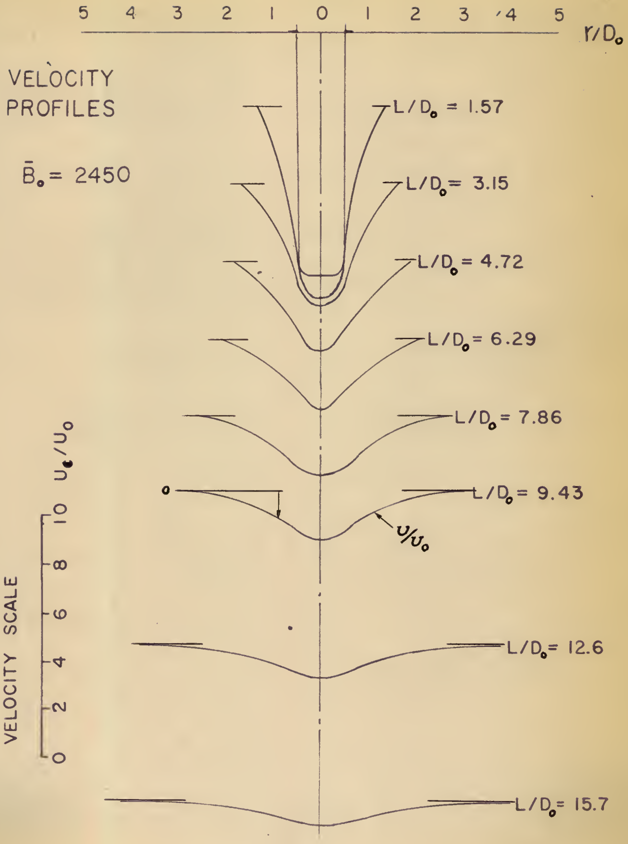
5 4 3 2 1 0 1 2 3 4 5
r/Do
VELOCITY PROFILES
B̄o = 2450
L/Do = 1.57
L/Do = 3.15
L/Do = 4.72
L/Do = 6.29
L/Do = 7.86
L/Do = 9.43
L/Do = 12.6
L/Do = 15.7
o
U/Uo
Uc/Uo
10
8
6
4
2
0
VELOCITY SCALE

VIII and IX. In Plate VIII, the velocity profiles obtained at certain representative levels of each of the jets have been plotted on common dimensionless coordinates of U/U_c and r/h. When an error function of the form $U/U_c = e^{-k_1(r/h)^2}$ was employed to represent the profiles, the value of k_1 increased with distance from the outlet in orifice diameters. However, a single mean curve was drawn with $k_1 = 64$. This curve fitted quite well a curve presented by Yen and Helander with $k_1 = 69$ for heated air jets from a vertical discharge unit heater. Another means of representing the cross jet velocity profiles was tried using Forstall and Gaylord's representation, $U/U_c = e^{-k_2(r/r_n)^2}$. The result is shown in Plate IX with the curve plotted on coordinates of U/U_c and r/r_n, where r_n is the value of r where the respective value of U/U_c reached ½ as explained in Fig. 1, Plate I. In the plot of Plate IX, as the abscissa was changed from r/h in Plate VIII to r/r_n in Plate IX, the band of data shrank to form a single curve which satisfactorily agreed with that presented by Forstall with $k_2 = 0.694$. The error function curve has been commonly used by investigators of non-buoyant jets and in the form $U/U_c = e^{-k(r/r_n)^2}$ would seem, from the foregoing, to be applicable to buoyant jets. Fig. 1, Plate X is a graph of velocities along the vertical axis of the jet plotted against distance from the outlet in outlet diameters. In order to match the equation

$$U_c/U_o = \left(\frac{h_p}{h}\right)\left[\frac{1 - (h/h_m)^2}{1 - (h_p/h_m)^2}\right]^n$$

the empirical factors n and h_p were obtained by a cut and trial

EXPLANATION OF PLATE VIII

Composite plot of all velocity profiles for jet from 0.159-inch nozzle with $\bar{B}_o = 2450$ and $\bar{B}_o = 1568$. Based on the error curve function $U/U_c = e^{-k_1(r/h)^2}$. The value of k increases with L/D_o. For the mean curve plotted in this plate, $k_1 = 64$.

PLATE VIII

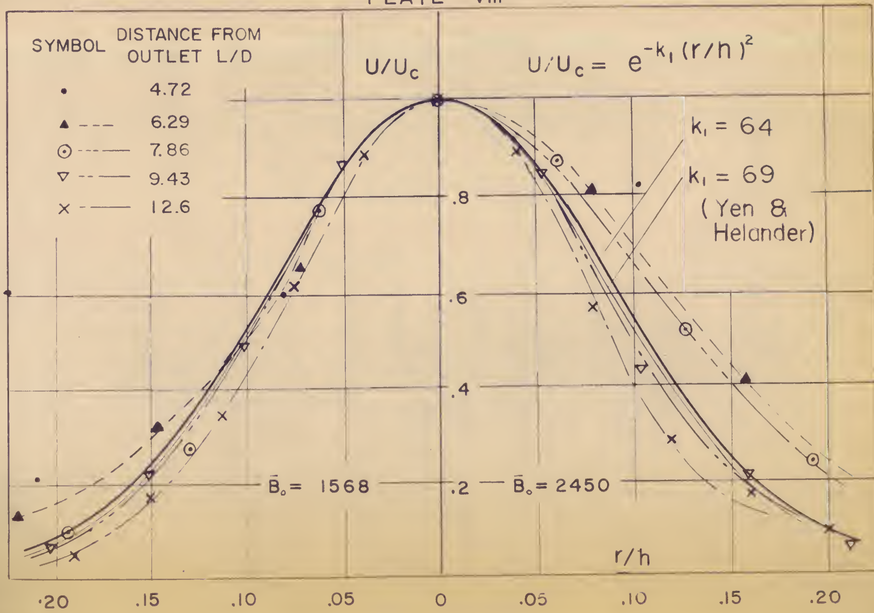
SYMBOL DISTANCE FROM OUTLET L/D
• 4.72
▲ 6.29
⊙ 7.86
▽ 9.43
× 12.6
U/U$_c$
U/U$_c$ = $e^{-k_1 (r/h)^2}$
k$_1$ = 64
k$_1$ = 69
(Yen & Helander)
.8
.6
.4
.2
B̄$_o$ = 1568
B̄$_o$ = 2450
.20
.15
.10
.05
0
r/h

EXPLANATION OF PLATE IX

Same as Plate VIII. Based on $U/U_0 = e^{-k_2(r/r_n)^2}$

The spread of points in Plate VIII shrank to form a single curve which satisfactorily agreed with that presented by Forstall with $k_2 = 0.694$.

PLATE IX

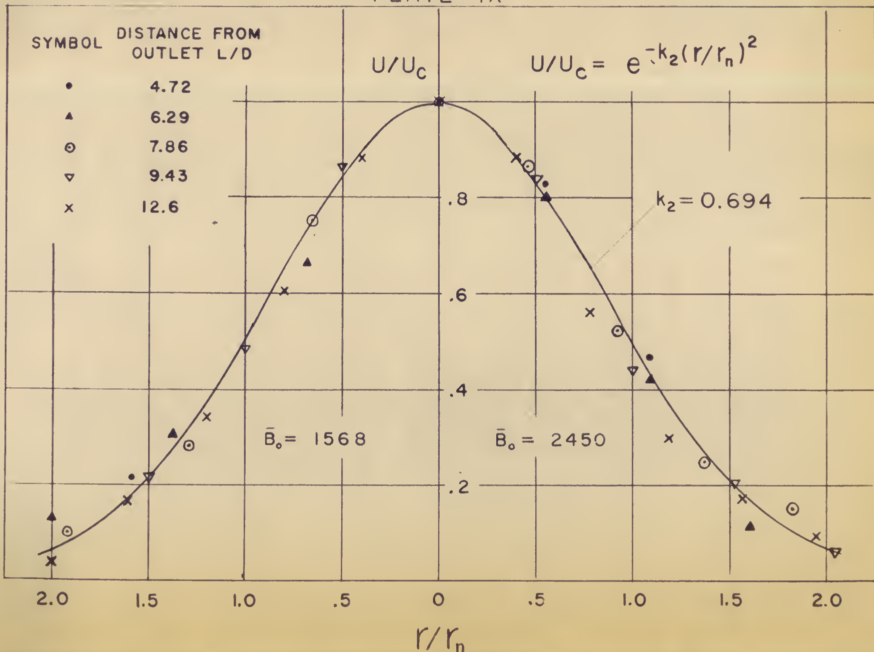
SYMBOL
DISTANCE FROM OUTLET L/D
4.72
6.29
7.86
9.43
12.6
U/U$_C$
U/U$_C$ = $e^{-k_2(r/r_n)^2}$
k_2 = 0.694
.8
.6
.4
.2
$\bar{B}_o$ = 1568
$\bar{B}_o$ = 2450
2.0
1.5
1.0
.5
0
.5
1.0
1.5
2.0
r/r$_n$

EXPLANATION OF PLATE X

Fig. 1. Ratio of velocity along the axis of jet to velocity at outlet.

Fig. 2. Ratio of temperature elevation along the axis of jet to temperature elevation at outlet.

PLATE X

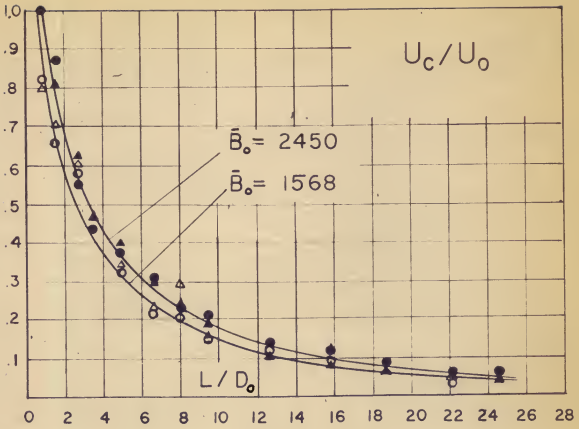

Fig. 1

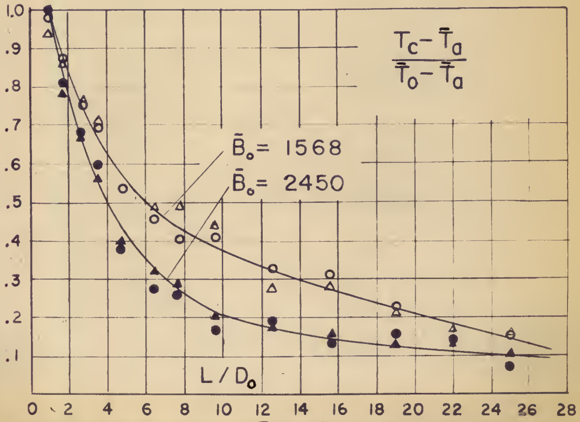

Fig. 2

method. With $n = \frac{1}{2}$ for both cases and $h_p/D_o = 1.88$ for the case where $\bar{B}_o = 2450$ and $h_p/D_o = 1.7$ for the case where $\bar{B}_o = 1568$, the equation matched the experimental data quite well.

From the foregoing, it would appear that the same correlating equation can be used for both water and air. Thus, it is apparent that the ratio of the center-line velocity U_c to the average velocity at the nozzle outlet U_o for the water jet as well as for the air can be represented by a function of three factors. These factors are: (1) h_p, the distance from an imaginary point source to a point where the principal zone begins; (2) h, the distance from the same imaginary point source to the level of the point under consideration; and (3) h_m, the distance from the imaginary point source to the bottom of the jet.

Temperature Profiles

Fig. 2, Plate X shows temperature along the vertical axis of the jet plotted against the distance down from the outlet in outlet diameters. The curve for the water jet as well as for the air jet can be represented by the equation

$$\frac{T_c - \bar{T}_a}{\bar{T}_o - \bar{T}_a} = \frac{h_p'}{h'} = \frac{h_p'/D_o}{L/D_o + h_o'/D_o}$$

The manner in which h_p'/D_o and h_o'/D_o were evaluated is illustrated in Plate XI. The values obtained are listed in Table 2. Comparison of these values, $h_p'/D_o = 5.1$ for the case where $\bar{B}_o = 1568$ and $h_p'/D_o = 3.2$ for the case where $\bar{B}_o = 2450$, with those obtained by Knaak and the author using air showed good agreement between the

Table 1. Test conditions.

Diameter of the nozzle outlet = 0.159 inch.

	$\bar{B}_o$ = 2450	$\bar{B}_o$ = 1568
Avg. outlet vel., U_o fps	2.88	2.88
Avg. flow at outlet, lb./min.	1.48	1.48
Avg. outlet temp., °F.	111	125
Max. temp. elevation at outlet, °F.	33	47
Avg. reference temp. (avg. temperature of bath water along wall), °F.	78	78
Avg. temp. of water entering upper tank	66	68

Table 2. Test result.

	$\bar{B}_o$ = 2450	$\bar{B}_o$ = 1568
Throw, L_{max}, in inches	16.3	12.9
h_o/D_o	0.54	0.4
h_p/D_o	1.88	1.7
h_m/D_o	102.5	81.4
h_o'/D_o	1.9	3.9
h_p'/D_o	3.2	5.1
F_b by integration, lb.	0.00134	0.00166
Change of momentum flux, lb.	0.00219	0.00219
θ, Time for the jet establishment measured by movie, in sec.		10.4
θ, Time, same as above but calculated by formula (B), in sec.		9.86

EXPLANATION OF PLATE XI

In this plate, the reciprocal of the ordinate of Fig. 2, Plate X has been plotted against travel, L/D_o. In agreement with

$$\frac{\bar{T}_o - \bar{T}_a}{T_c - \bar{T}_a} = \frac{h'/D_o}{h'_p/D_o} ,$$

the points plotted are represented by the straight lines.

PLATE XI

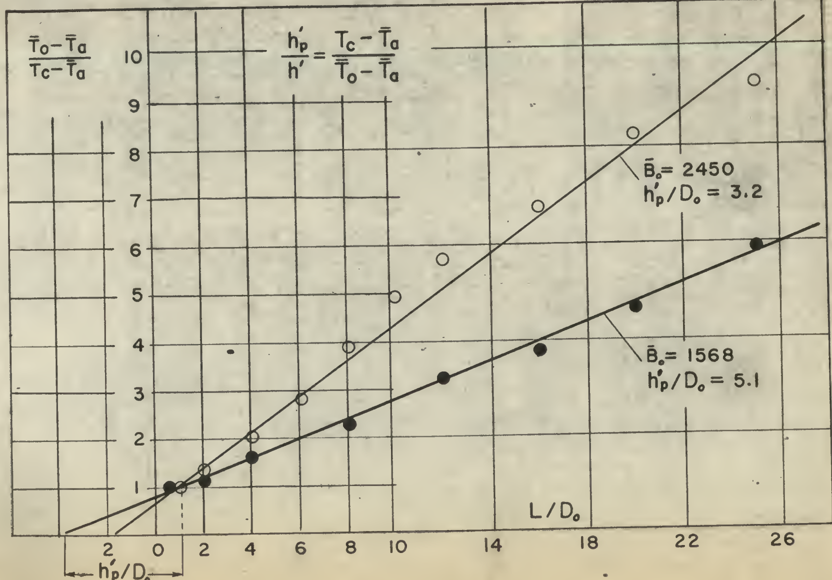

$\frac{\bar{T}_o - \bar{T}_a}{T_c - \bar{T}_a}$
$\frac{h'_p}{h'} = \frac{T_c - \bar{T}_a}{\bar{\bar{T}}_o - \bar{T}_a}$
10
9
8
7
6
5
4
3
2
1
$\bar{B}_o = 2450$
$h'_p/D_o = 3.2$
$\bar{B}_o = 1568$
$h'_p/D_o = 5.1$
L/D_o
2
0
2
4
6
8
10
14
18
22
26
h'_p/D_o

water jet and the air jet.

Buoyancy Force and Momentum Flux

The temperature profiles plotted in Plates XII and XIII were employed for evaluating the buoyancy force acting on the jets. As was pointed out before,

$$F_b = \int_0^{V_j'} (\rho_a - \rho)\, dV = \int_0^{L_m} \int_0^{V_j'} (\rho_a - \rho) \cdot 2\pi r (dr) dL$$

in order to carry out the multiple integration, the temperature profiles obtained at each representative level were replotted. The difference between the specific weights ρ_a and ρ was plotted against $(r)^2$, shown in Fig. 1 of Plate XIV as one example, to complete the first integration. The second integration was completed as shown in Fig. 2 of Plate XIV. The curves in this figure were developed by plotting the result of the first graphical integration against the distance L. By evaluating again the area under these second curves, the buoyancy force was computed.

The change of momentum flux for the jet was obtained as the product of the values of mass flow rate and the velocity at the nozzle outlet. Since there was no momentum flux leaving the system, the momentum flux that issued through the nozzle outlet was considered to be entirely dissipated inside the bath. The mass flow rate was obtained by measuring the average weight of the overflow from the tank in the given length of time. The change of momentum flux was found to be 0.00219 pound and the buoyancy force computed by graphical integration was found to be 0.00166 pound

EXPLANATION OF PLATE XII

Temperature Profiles

$\bar{B}_o = 1568$

PLATE XII

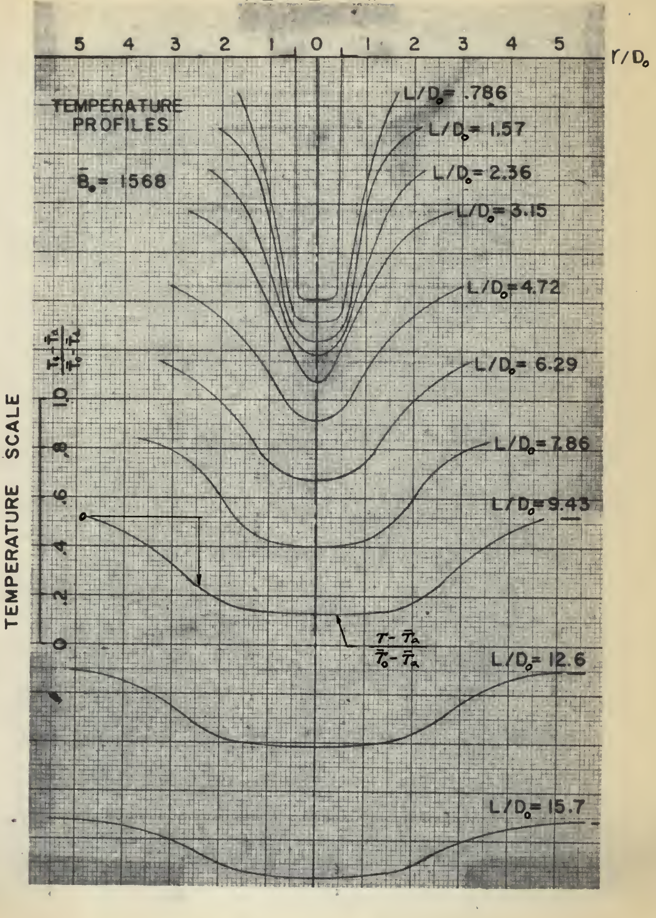

5 4 3 2 1 0 1 2 3 4 5
r/D_o
TEMPERATURE PROFILES
B_o = 1568
L/D_o = .786
L/D_o = 1.57
L/D_o = 2.36
L/D_o = 3.15
L/D_o = 4.72
L/D_o = 6.29
L/D_o = 7.86
L/D_o = 9.43
L/D_o = 12.6
L/D_o = 15.7
TEMPERATURE SCALE
0 .2 .4 .6 .8 1.0
$\frac{T_t - \bar{T}_a}{\bar{T}_o - \bar{T}_a}$
$\frac{T - \bar{T}_a}{\bar{T}_o - \bar{T}_a}$

EXPLANATION OF PLATE XIII

Temperature Profiles

$\bar{B}_o = 2450$

PLATE XIII

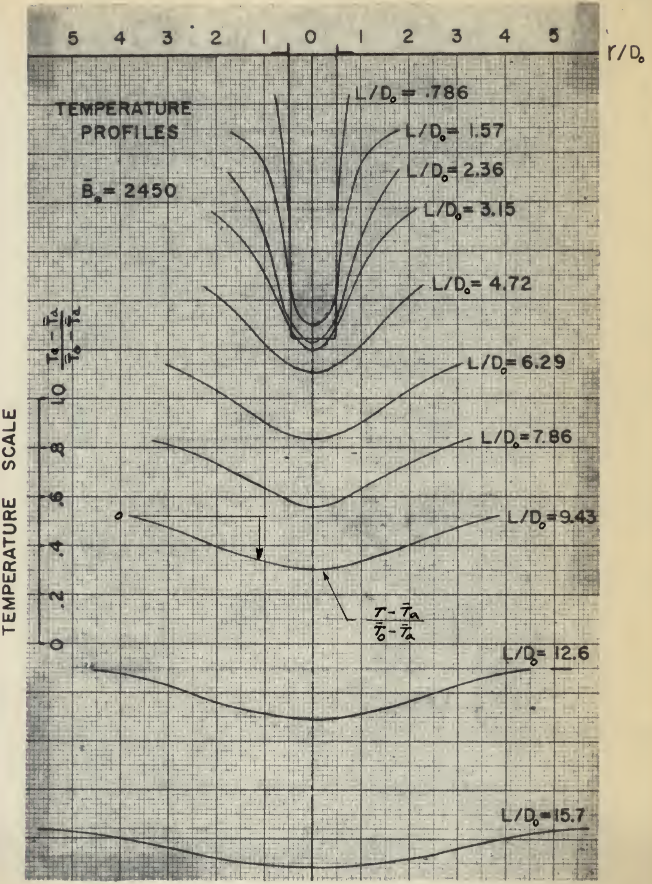

5 4 3 2 1 0 1 2 3 4 5
r/D₀
TEMPERATURE PROFILES
B̄₀ = 2450
L/D₀ = .786
L/D₀ = 1.57
L/D₀ = 2.36
L/D₀ = 3.15
L/D₀ = 4.72
L/D₀ = 6.29
L/D₀ = 7.86
L/D₀ = 9.43
L/D₀ = 12.6
L/D₀ = 15.7
TEMPERATURE SCALE
0 .2 .4 .6 .8 1.0
(T₀ − T̄ₐ)/(T̄₀ − T̄ₐ)
(T − T̄ₐ)/(T̄₀ − T̄ₐ)

EXPLANATION OF PLATE XIV

Fig. 1. An example of the first integration carried out by the graphical method

$$\text{Area} = \int_0^{r'_j} (\rho_a - \rho) \cdot d(r)^2 = f$$

Fig. 2. Second integration

$$\pi \cdot \text{Area} = \pi \int_0^{L'_m} f \cdot dL = \int_0^{L'_m} \int_0^{r'_j} (\rho_a - \rho) \cdot 2\pi r(dr) \cdot dL$$

$$= F_b$$

PLATE XIV

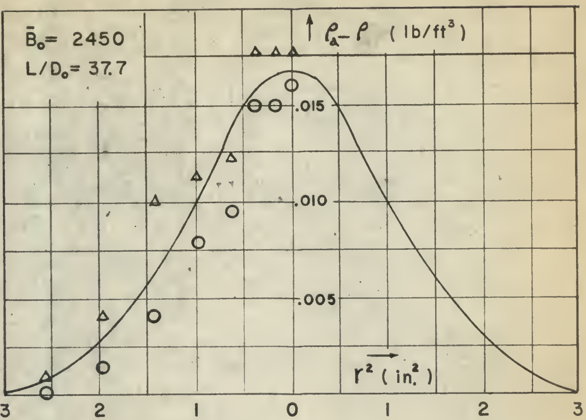

Fig. 1

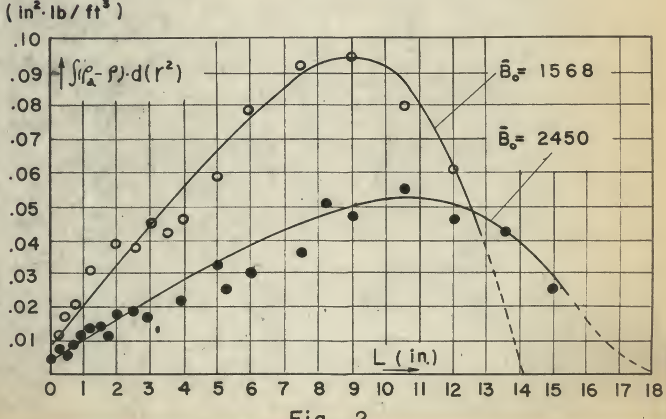

Fig. 2

for the case of $\bar{B}_0$ = 1568 and 0.00134 pound for the case of $\bar{B}_0$ = 2450. The result was not in agreement with the theory, which requires that the buoyancy force has to be equal to the change of the momentum flux. Whether this discrepancy was due to some other effects unaccounted for or whether experimental error was involved, is not known. It is to be noted that near the bottom of the jets where the temperature elevations were so small as to be difficult to detect, the measured values were of doubtful accuracy.

Jet Boundaries

Plate XV shows the jet boundaries which were studied by a shadow graph like that represented by Plate XVI. The jet boundary obtained by means of the shadow graph was much more accurate than that obtained by means of a pitot-tube determination of the surface of zero downward velocity, because the shadow graph made visible the jet motion as well as the jet boundary. As in the case of the air jet, the jet becomes smaller with the smaller buoyancy number. Outside the jet boundary, which was defined as a surface of zero downward velocity, there existed a region of elevated temperature. In this region, a turbulent upward flow of water occurred, induced by the elevated temperature. The jet boundaries of zero temperature elevation are also shown in Plate XV. The buoyancy forces were computed with this zero temperature surface as the boundary of the integration.

EXPLANATION OF PLATE XV

Jet boundaries determined from velocity and temperature profiles by shadow graphs. Diameter of nozzle outlet was 0.159 inch and the temperature elevation at the outlet was 33° F. for $\bar{R}_0$ = 2450 and 47° F. for $\bar{R}_0$ = 1568.

PLATE XV

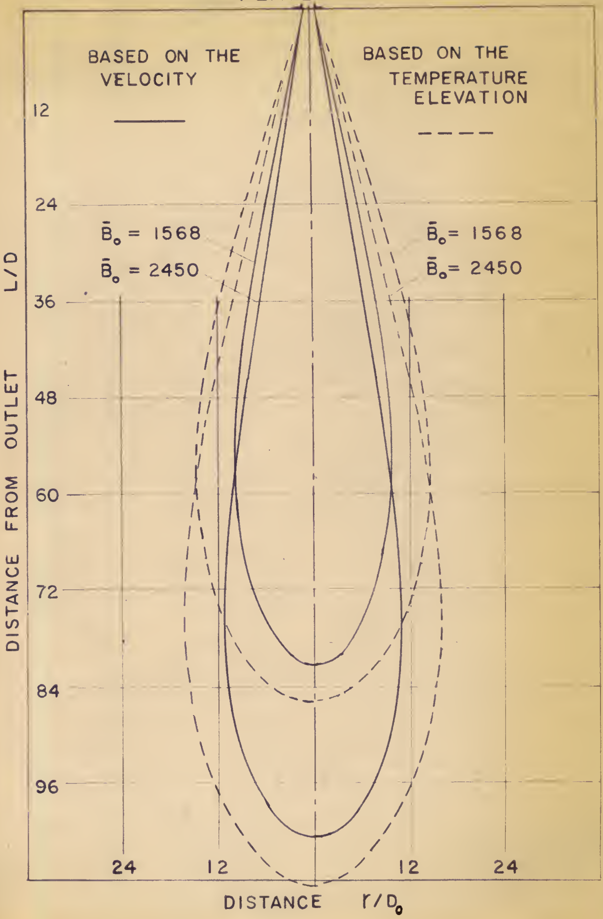
BASED ON THE VELOCITY
BASED ON THE TEMPERATURE ELEVATION
$\bar{B}_o$ = 1568
$\bar{B}_o$ = 2450
$\bar{B}_o$= 1568
$\bar{B}_o$= 2450
12
24
36
48
60
72
84
96
24
12
12
24
DISTANCE FROM OUTLET L/D
DISTANCE r/D$_0$

EXPLANATION OF PLATE XVI

Shadow graph showing the shape of the jet.

PLATE XVI

Time Study for the Jet Establishment

As stated before, the time required to establish a complete jet boundary can be evaluated by the equation:

$$\theta = \frac{U_o}{g\left(\frac{\rho_a - \rho_o}{\rho_o}\right)} \text{ ----------------- (B)}$$

By the data obtained in this experiment, the calculated θ was 9.86 seconds. Motion pictures employ both shadow graphs and colored jets, and the length of time required to establish the jet is measured as 10.4 seconds. This agreed quite well with the equation, which in turn verified the assumption that the buoyancy force is equal to the change of momentum flux.

DISCUSSION AND RECOMMENDATIONS

Difficulties with Water

There were two main difficulties involved with water as a test medium. First, it was not easy to get higher heads with the simple equipment used; and second, it was not easy to obtain low values of the buoyancy number because the change of density due to heating was not large for the water.

Accuracy in the Experiment

(1) Due to the small diameter of the nozzle, which was merely 0.159 inch, even a slight inaccuracy in locating an instrument in the jet, could in the vicinity of the outlet cause a large error. Some inaccuracy in positioning the thermocouple and the

pitot tube was inevitable with the equipment used, especially at a level near the nozzle outlet where a possible error of 1/64 inch in its location caused an error equal to nearly 10 per cent of the orifice diameter. For example, at the level of L/D_o = 2.34 where the velocity profile reached only to r/D_o = 1.3, an error of 0.1 r/D_o was quite a large value. (2) Various investigators have found that the principal zone begins at a distance of approximately 5 nozzle diameters below the nozzle outlet. In the author's experiment, L_p, the distance from the orifice to the point of the beginning of the principal zone, was found to be only one orifice diameter. This result seems to be too small. The nozzle diameter was so small that the relative size of the pitot tube was too large for an accurate measurement at levels near the jet outlet. This relatively large pitot tube could have caused choking of the flow. Also, measured values were not representative of point values but were average values over an area equal to the diameter of the pitot tube. (3) The heat-releasing capacity of the tank containing the bath water was too small and the temperature of the bath never reached a fixed value. This made the experiment very difficult because the temperature elevations were based upon the temperature of the bath water. The arrangements to eliminate the bad effects of this unsteady state were discussed in the former chapter. (4) As was pointed out before, the measurement of small velocity heads in the water was very difficult. There is a need to develop some other technique for this purpose. (5) For further experiments, it is recommended therefore that a much larger tank with a bigger nozzle be used and that many thermocouples inside and outside of the jet boundary be installed. This would permit the temperature distribution to be recorded at once by a high-speed, electronic, curve-drawing instrument and the bad effects due to the unsteady temperature distributions would be the more nearly eliminated. (6) The water tank should be reconstructed with both front and back walls of glass. The front glass should be transparent and the back one translucent. If two lights[1] are then used to illuminate the jet through the back glass, the shadow graph will appear much more distinct. Further studies of the jet motion and the boundary condition, either by motion picture or by observations, will be more successful by this arrangement.

CONCLUSIONS

Though some inaccuracies were involved in this experiment, the following points were quite apparent.

(1) The diffusion of velocity and temperature in an axially symmetric heated water jet is like that in a heated air jet.

(2) Those equations used in heated air jets to represent its velocity or temperature distributions can be used in heated water jets quite well.

(3) The employment of the experimental constant in the error function for air jets obtained by Yen and Helander is justified experimentally for water jets by this research.

(4) The thermal effect of the jet extended outside the jet

---

[1]It is required that the lights must not be seen directly from the front.

boundary which was defined as a surface of zero vertical velocities. The boundary surface of zero temperature elevation with respect to the surrounding water had a much bigger radius than the boundary surface of zero downward velocity and was very unsteady because of the high turbulence. However, a line of constant temperature elevation drawn in the vicinity of the jet had the shape of the jet.

(5.) The time study of the jet boundary establishment indicated that the change of momentum flux of the jet was nearly equal to the buoyancy force induced by the heated jet. Yet, from the result obtained by the direct integration of the buoyancy forces, the change of momentum flux was found to be nearly 1.4 times the buoyancy force. This needs to be investigated further, using much more accurate and complete equipment.

NOMENCLATURE

L Vertical coordinate from the orifice.

h Vertical coordinate from the imaginary point source.

h_o Distance between imaginary point source and origin.

$\bar{B}_o$ Cross-stream average buoyancy number at outlet.
$(U_o^2/g.D_o)/(\rho_a/\rho_o - 1)$

D_o Outlet diameter.

g Gravitational acceleration, 32.2 ft./sec.^{2}

g_c Conversion factor, 32.2 lb. - m.·ft./lb. - f·sec.^{2}

r Radial distance from axis of jet to point of jet under consideration.

r_j Radial distance from axis of jet to point of outside jet boundary established as surface of zero downward velocity.

r_n Radial distance where the respective value of U/U_c reached ½ as explained in Fig. 1, Plate I.

T Temperature.

θ Time in sec.

M_o Mass rate of flow at outlet, lb./sec.

U Local velocity, ft./sec.

Specific weight, lb./ft.^{3}

W Weight of water contained in the main tank, lb.

A Base area of the main tank, ft.^{2}

Y Height of water contained in the bath, ft.

D_v Volumetric diffusivity.

μ Viscosity.

P_a Atmospheric pressure, lb./ft.^{2}

F_b	Buoyancy force induced by the heated jet, lb.
k_1, k_2, C	Constants to be used in an error function for the velocity distributions.
X	Variable (r/r_n) or (r/h) to be used in an error function.
e	Natural logarithm.
V	Volume.
V_j	Volume confined within the jet velocity boundary.
V_j'	Volume confined within the jet temperature boundary.
V_b	Volume for the tank.
m	Subscript, indicates values at the end of the jet.
o	Subscript, indicates values at the orifice.
p	Subscript, indicates values at the beginning of principal zone.
a	Subscript, indicates values of surrounding fluid.
c	Subscript, indicates values on the axis of the jet.
-	Denotes mean values.
′	Denotes values based on temperature.

ACKNOWLEDGMENTS

The writer wishes to express his appreciation to Professor Linn Helander for his guidance and suggestions. Acknowledgment of appreciation is also due to Professor R. E. Crank, who made many valuable suggestions on measurement techniques. The writer is indebted to Dr. R. G. Nevins and Dr. S. M. Yen for their kind assistance.

REFERENCES

(1) Albertson, M. L., Y. B. Dai, R. A. Jensen and Hunter Rouse. Diffusion of submerged jets, p. 1573.

(2) Corrsin, Stanley. Investigation of flow in an axially symmetrical heated jet of air, p. 3.

(3) Forstall, W. and E. W. Gaylord. Momentum and mass transfer in a submerged water jet. Journal of Applied Mechanics, p. 161-164. June, 1955.

(4) Helander, Linn and C. V. Jackowatz. Downward projection of heated air. ASHVE Transactions, p. 71-77, Vol. 54. 1948.

(5) Helander, Linn, Shee-Mang Yen and R. E. Crank. Maximum downward travel of heated air jets from standard long radius ASME nozzle. ASHVE Journal Section Heating, Piping and Air Conditioning, p. 123-132. March, 1953.

(6) Helander, Linn, Shee-Mang Yen and C. B. Knee. Characteristics of downward jets of heated air from a vertical discharge unit heater. Journal Section Heating, Piping and Air Conditioning, p. 149-155. Nov., 1955.

(7) Knaak, Ruediger and Hwachii Lien. Study of heated and unheated air jet with various buoyancy numbers. An unpublished report to the M. E. Dept., Kansas State College.

A MODEL STUDY OF BUOYANT JETS

by

HWACHII LIEN

B. S., National Taiwan University, Taipei,
Taiwan, China, 1953

AN ABSTRACT OF A THESIS

submitted in partial fulfillment of the

requirements for the degree

MASTER OF SCIENCE

Department of Mechanical Engineering

KANSAS STATE COLLEGE
OF AGRICULTURE AND APPLIED SCIENCE

1956

ABSTRACT

The purpose of this research was to investigate the characteristics of a jet of heated water projected vertically downward into a bath of unheated water, and to relate these to corresponding data on downwardly projected jets of heated air. Specifically, the objectives of the study were to (1) obtain data descriptive of the behavior of the downwardly projected jet of heated water, (2) investigate the establishment and location of the jet boundary by the shadow graphs or potassium per manganese technique, (3) compare the data or downthrow of water jets to that of the air jets, (4) find out the buoyancy force of the water jet by graphical integration and check with the change of momentum flux at the jet, (5) obtain guidance for further research.

Two separate runs, for $\bar{B}_0$ = 1568 and $\bar{B}_0$ = 2450, with duplicate measurements for each point gave data from which the temperature and velocity profiles were plotted. These plots of the temperature and the velocity distributions for the heated water jets were compared to those for the heated air jets. Whether or not the same equation to represent its velocity or temperature distributions can be used both for air jets and water jets was studied. The jet boundaries were traced quite accurately by means of shadow graphs. Also, two different ideas were applied to determine whether or not the change of momentum flux equaled the buoyancy force. The two methods introduced were direct integration and time study for the establishment of the fully developed jet boundary.

The similarity of the water jet to the air jet was evident. The conclusions obtained from this research were:

(1) Those equations used in heated air jets to represent their velocity or temperature distributions can be used in heated water jets.

(2) The employment of the experimental constant in the error function for air jets obtained by other investigators was justified experimentally for water jets by this research.

(3) The thermal effect of the jet extended outside the jet boundary, which was defined as a surface of zero vertical velocities. The line of zero temperature elevation with respect to the surrounding water had a much bigger radius than the downward jet and was very unsteady because of the high turbulence. However, a line of constant temperature elevation drawn in the vicinity of the jet had the shape of the jet.

(4) It will be concluded by the time study of the jet boundary establishment that the change of momentum flux of the jet is nearly equal to the buoyancy force induced by the heated jet. Yet, from the result obtained by the direct integration of the buoyancy forces, the change of momentum flux was nearly 1.4 times the buoyancy force induced. This needs to be investigated further experimentally, using much more accurate and complete equipment.